Cooperation between T cell receptor and Toll-like receptor 5 signaling for CD4 + T cell activation

Otoniel Rodríguez-Jorge, Linda Kempis-Calanis, Wassim Abou-Jaoudé, Darely Gutiérrez-Reyna, Céline Hernandez, Oscar Ramirez-Pliego, Morgane Thomas-Chollier, Salvatore Spicuglia, Maria Santana, Denis Thieffry

Cooperation between T cell receptor and Toll-like receptor 5 signaling for CD4$^+$ T cell activation

Otoniel Rodríguez-Jorge[1,4], Linda A. Kempis-Calanis[1], Wassim Abou-Jaoudé[2], Darely Y. Gutiérrez-Reyna[1], Céline Hernandez[2], Oscar Ramirez-Pliego[1], Morgane Thomas-Chollier[2], Salvatore Spicuglia[3], Maria A. Santana[1]*, Denis Thieffry[2]*

[1]Centro de Investigación en Dinámica Celular. Instituto de Investigación en Ciencias Básicas y Aplicadas. Universidad Autónoma del Estado de Morelos. 62210 Cuernavaca, México.
[2]Computational System Biology team. Institut de Biologie de l'Ecole Normale Supérieure. CNRS UMR8197. INSERM U1024. École Normale Supérieure. Université PSL. 75005 Paris, France.
[3]Aix-Marseille University. Inserm. TAGC. UMR1090. 13288 Marseille, France.
[4]Escuela de Estudios Superiores de Axochiapan. Universidad Autónoma del Estado de Morelos. 62951 Axochiapan, México

*Corresponding authors. Email: santana@uaem.mx (M.A.S.); denis.thieffry@ens.fr (D.T.)

Abstract

CD4$^+$ T cells recognize antigens through their T cell receptors (TCRs); however, additional signals involving co-stimulatory receptors, for example CD28, are required for proper T cell activation. Alternative co-stimulatory receptors have been proposed, including members of the Toll-like receptor (TLR) family, such as TLR5 and TLR2. To understand the molecular mechanism underlying this co-stimulatory function, we generated detailed molecular maps and logical models for the TCR and TLR5 signaling pathways, together with a merged model accounting for cross-interactions. Furthermore, we validated the resulting model by analyzing the responses of T cells to the activation of these pathways alone or in combination, in terms of the activation of the transcriptional regulators CREB, AP-1 (c-Jun), and NF-κB (p65). Our merged model accurately reproduces the experimental results, showing that the activation of TLR5 can play a similar role to that of CD28 activation with respect to AP-1, CREB, and NF-κB activation, thereby providing insights regarding the cross-regulation of these pathways in CD4$^+$ T cells.

Introduction

Antigens are presented to $CD4^+$ T cells by specialized antigen-presenting cells (APCs), such as dendritic cells, through major histocompatibility complex (MHC) class II molecules. $CD4^+$ T cells recognize the antigens through their T cell receptors (TCRs) (1–4). These cells also receive signals through the co-receptor CD4, co-stimulatory receptors, such as CD28, and through other stimulatory and inhibitory accessory receptors (5–7). These receptors sense the cytokines and other molecules in the microenvironment surrounding the cells and on the surface of the APCs. T cells integrate these signals, which results in their activation and differentiation into specialized effector cells (7–11). $CD4^+$ T cells coordinate the adaptive immune response through cell-to-cell contacts and the secretion of cytokines that influence the activity of other cell types. TCR signaling has been a major research topic during the last decade, in particular with a view to identifying new targets to inhibit, enhance, or alter the outcome of T cell activation. However, an updated comprehensive version of this crucial pathway is missing. In recent years, new, high-throughput technologies have enabled substantial advances in the field, revealing an unprecedented level of complexity of TCR signaling (12–18).

TCR-mediated signaling can be divided in four main modules: (i) early signaling, which is characterized by the recruitment and phosphorylation of Lck (Lymphocyte cell-specific protein-tyrosine kinase); (ii) the formation of signalosome complexes containing LAT (Linker for activation of T-cells), CD6 (T-cell differentiation antigen CD6), or both; (iii) the activation of important mediators such as protein kinase C θ (PKCθ); and (iv) downstream signaling through mitogen-activated protein kinases (MAPKs), inhibitor of nuclear factor kappa-B kinases (IKKs) kinases, and Ca^{2+}-mediated signaling (19–22). TCR signaling results in the activation of inducible

transcription factors, which in turn promote changes in gene expression. The main transcription factors that mediate TCR-inducible gene expression are: NFAT (Nuclear Factor of Activated T cells), NF-κB (Nuclear Factor kappaB), AP-1 (Activator protein 1), and CREB (cAMP Response Element Binding) (20, 23–28). A proper balance between the activation of these transcription factors leads to robust T cell activation and differentiation, whereas imbalances may induce an impaired immune response, which can result in anergy or apoptosis (4, 29–32). For example, NF-κB and NFAT are both members of the Rel family of transcription factors and may compete for binding motifs on DNA targets. A balance between NFAT and NF-κB affects the phenotype of the cells. When NF-κB activity is greater than that of NFAT, the cell exhibits a proinflammatory response, whereas the absence of NF-κB activity leads to an anti-inflammatory response (33–36). Other transcription factors that respond to TCR activation include β-catenin (37, 38) and serum response factor (SRF) (39).

T cell activation takes place in the lymph nodes where, in addition to the signals provided by APCs, pieces of antigens and molecules secreted by other cells circulate. Among these, the flagellin monomer is directly recognized by $CD4^+$ T cells through the cell-surface receptor TLR5 (40, 41). TLRs are important modulators of the cellular response and triggering their activation through appropriate vaccine adjuvants is a promising therapeutic approach. TLR expression, signaling, and function have been characterized in cells of the innate immune system (42–45). TLR signaling is initiated by ligand binding, dimerization of receptors, and recruitment of the adaptor proteins MyD88 (Myeloid differentiation primary response protein MyD88) or TRIF (Toll-interleukin-1 receptor domain-containing adapter inducing interferon beta). With the exception of TLR3, all TLRs recruit MyD88, whereas TLR3, TLR4, and TLR5 recruit TRIF. These adaptors induce the

sequential recruitment and activation of a series of kinases of the IRAK (Interleukin-1 receptor-associated kinase) family, leading to the activation of IKKs and MAPKs (45–48). The activation of TLRs can also stimulate the phosphatidylinositol 4,5-bisphosphate 3-kinase (PI3K) pathway, leading to the activation of the transcription factors AP-1 and CREB (49–51). Together, downstream of TLR signaling, NF-κB, AP-1, and CREB are activated. When TLRs recruit TRIF, members of the interferon response factor (IRF) family of transcriptional regulators are also activated (52, 53).

Flagellin, a component of the flagella of many bacteria and a ligand of TLR5, has been proposed as a vaccine adjuvant for its ability to induce a proinflammatory response in several cell types (54–57). Although classically studied for its function in cells of the innate immune system, TLR5 is one of the main TLRs expressed in T cells. In $CD4^+$ T cells, TLR5 function is not well characterized, but it was reported that TLR5 co-stimulatory signals can induce proliferation and expression of cytokines, such as interferon- γ (IFN-γ) (58). Moreover, $CD4^+$ and $CD8^+$ T cells respond to TLR5 co-stimulatory signals (59, 60).

To better understand the role of TCR signaling network in the activation of key transcription factors, focusing in particular on the interplay between TCR and TLR5-mediated signaling, we have used two complementary computational approaches to generate (i) detailed molecular maps of the TCR and TLR5 pathways, and (ii) predictive qualitative models of the dynamical behavior of these pathways, taking into account documented cases of cross-talk. To build and refine these models, we took advantage of the RNA-seq and ChIP-seq data generated by the BLUEPRINT consortium (http://www.blueprint-epigenome.eu/). Furthermore, we evaluated the activation of c-

Jun, p65, and CREB upon engagement of the TCR in the absence or presence of the TLR5 ligand, flagellin. Model predictions were systematically compared with experimental data to refine and validate our models. Our combined experimental and modeling analyses indicate that TLR5 is a co-stimulatory receptor of the TCR, with an effect on cell activation comparable to that of CD28.

Results

Generation of a molecular map and a logical model for the TCR pathway

We collected information from public databases, in particular Reactome and KEGG, and curated the literature to construct a molecular map describing the TCR signaling network (Fig. S1 and File 1). Using the software GINsim (http://ginsim.org), we then built a detailed logical model describing TCR-mediated signaling in $CD4^+$ T cells, taking as starting point the model published by Sáez-Rodriguez *et al* (61), and substantially updating it with data previously integrated in the molecular map. We used mainly data from primary human and mouse $CD4^+$ T cells, which were completed with information from human $CD8^+$ T cells, as well as from Jurkat cells and other cell lines, assuming that key signaling events are conserved between T cells, and furthermore between mice and humans. The model nevertheless keeps track of the origin of the information (cell lines, species, and bibliographical entries) in the annotations associated with each component. To ensure that all model components were effectively expressed in $CD4^+$ T cells, we checked their expression using public RNA-seq and ChIP-seq data (Table S1 and Materials and Methods). The resulting TCR-mediated signaling model encompasses 110 nodes (Fig. 1 and File 2). In particular, TCR and CD28 correspond to the canonical receptors that initiate the activation of $CD4^+$ T cells (represented by green nodes in Fig. 1). Other nodes, such as CD4, CD45, CD6, RCAN1, and Akap5, correspond to model inputs for which we considered a default value of 1 or 0 (see Table S5). In vivo, TCR

signals are provided by an antigenic peptide presented by APCs in association with MHCII molecules. CD4 recognizes the MHCII molecule itself, and CD28 recognizes the co-stimulatory molecules (CD80 and CD86) expressed in activated APCs.

We included the key transcription factors NF-κB (NFkB in the model and in Fig. 1), AP-1 (AP1), NFAT (NFAT), CREB (CREB1), SRF (SRF) and β-catenin (CTNNB1) (Fig. 1, yellow nodes). A combination of these transcription factors regulates most of the effector genes expressed during $CD4^+$ T cell activation. To facilitate interpretation, we further explicitly included phenotypic nodes (Fig. 1, output nodes in gray) representing functional responses: proinflammatory cytokines (PICytokines), anti-inflammatory cytokines (AICytokines), cell cycle progression (CellCycleProg), survival (Survival), cytoskeleton re-arrangement (ActinRem), and anergy (Anergy). The model was then completed by assigning a logical rule to each node (Table S2). These logical rules describe how the activation status of each node is determined by the amounts of its regulators (see Materials and Methods). We computed the stable states of the TCR model and compared them with the experimental behavior of the TCR pathway as reported in the literature. Observed discrepancies led us to refine the model rules (see Supplementary Text) until a reasonable qualitative match was obtained (see Fig. 2). For example, stimulation of the TCR alone induces NFAT activation and a state of anergy, whereas stimulation of both the TCR and CD28 induces the activation of NFAT, NF-κB, AP-1, and CREB, promoting cytoskeleton re-arrangement, survival, cell cycle progression, and the expression of pro- and anti-inflammatory cytokines. Next, we assessed the behavior of our model in the context of either knockout or inhibition of PI3K (PI3K) or PKCθ (PKCth). The model correctly reproduces several scenarios. First, when only TCR signals are present (without co-stimulation), a state of anergy is reached,

which is characterized by the activation of NFAT and the lack of AP-1 and NF-κB activation. Second, when both the TCR and CD28 are stimulated, all six transcription factors are activated. Third, when PI3K activity is impaired, the activation of AP-1 and NF-κB is compromised (which would lead to anergy). This occurs because PI3K contributes to the activation of NF-κB (62) and AP-1 (63). Fourth, our model accounts for the fact that NF-κB cannot be activated by TCR signals (either alone or in combination with CD28 signals) when PKCθ is impaired, due to the lack of proper activation of IKK (23, 64). In this case, our model predicts that the production of proinflammatory cytokines, cell cycle, and survival, for which NF-κB is essential, would be affected when this transcription factor is not activated, but that the production of anti-inflammatory cytokine would be unaffected.

Generation of a molecular map and a logical model for TLR5 pathway

Similarly, to study the role of TLR5 signaling in naïve $CD4^+$ T cells, we generated a detailed molecular map (Fig. S2 and File 3) and a logical model (Fig. 3 and File 4) for this pathway. Our TLR5 logical model encompasses 42 nodes, including one input component, TLR5, which is activated by flagellin. The model further includes the transcription factors NF-κB (NFkB), AP-1 (AP1), and CREB (CREB1), together with three phenotypic (output) nodes representing proinflammatory cytokines (PICytokines), anti-inflammatory cytokines (AICytokines), and cell survival (Survival). As for the TCR model, we used transcriptomic and epigenetic data from BLUEPRINT consortium (Table S1) to verify the expression of the signaling molecules. We kept only those components associated with active enhancers (H3K4me1 and H3K27ac marks) and/or active promoters (H3K4me3 and H3K27ac marks), together with statistically significant gene expression as reported in the RNA-seq data (Fig. S3). Finally, a logical rule was assigned to each

node of the TLR5 regulatory graph (Table S3) as for the TCR model (see Materials and Methods). To challenge our TLR5 model (Fig. 3), we compared model simulations with published experimental data for the wild-type situation, as well as for TAK1 and PI3K knockouts (Fig. 4). The simulation of the TAK1 KO resulted in the loss of activation of NF-κB, AP-1, and CREB, as observed previously (49, 65–68). Similarly, simulation of the PI3K KO resulted in the impairment of NF-κB, AP-1, and CREB activation, consistent with previous studies (62, 63, 69, 70).

Cooperation between TCR and TLR5 signals for T cell activation

To analyze the interactions between TCR and TLR5 pathways and their role in T cell activation, we merged our TCR and TLR5 models using the GINsim software (Fig. 5, Table S4 and File 5). Our merged model encompasses 128 nodes, including three externally controlled inputs (TCR, CD28, and TLR5) and six phenotypic (output) nodes. Although both receptors coincide in the activation of common transcription factors, the signaling pathways leading to transcription factor activation are mostly independent.

Next, we computed the stable states of the resulting model for wild-type and mutant backgrounds and adjusted the rules of the components lying at the intersection between the two original models to consider all regulatory inputs and to be consistent with the experimental data (Fig. 6; see the Supplementary Text for more details on the adjustment of the logical rules). Taking advantage of a model reduction functionality implemented in GINsim (see Materials and Methods), we generated a simpler, but dynamically consistent, version of the merged "TCR+TLR5" model, which conserves all critical nodes and interactions (Fig. S4). The reduced merged model encompasses 59 components. This model was then used to simulate T cell activation by different

combinations of signals. According to these simulations, TLR5 signals induce the activation of the PI3K, NF-κB, and MAPK pathways (Fig. 4). We hypothesized that this activation process could synergize with TCR signals to induce a productive activation of naïve $CD4^+$ T cells.

Experimental validation of the merged TCR and TLR5 model

To challenge our merged TCR+TLR5 model, we studied the response of naïve $CD4^+$ T cells to stimulation of the TCR alone, of TLR5 alone, of the TCR together with TLR5, and of the TCR together with CD28, in strong and weak activation conditions, and assessed the phosphorylation of p65, c-Jun, and CREB1. As strong stimulus, we used a high concentration (1 μg/ml) of each anti-CD3 and anti-CD28 antibody crosslinked with a goat anti-mouse antibody, as reported by others (71–75). We further used a lower concentration (0.1 μg/ml) of each antibody to achieve a weak or suboptimal stimulation (74–77). Although all the evaluated molecules showed a basal level of phosphorylation, statistically significantly greater phosphorylation was achieved when the cells were exposed to strong stimuli of TCR alone (for CREB activation), or of TCR and co-stimulatory signals (for p65 and c-Jun) (Fig. 7). Weak signals by the TCR or costimulatory molecules in different combinations resulted in wide variations in the extent of p65 and c-Jun activation, suggesting that signaling strength must exceed a threshold to result in robust activation of the cell population, which only under strong TCR stimulation and co-stimulation was reproducible in every biological sample. Furthermore, the combination of TCR and TLR5 stimulation gave rise to a similar response to that induced by costimulation of the TCR and CD28. Together, our experimental results thus suggest the potential of flagellin to provide co-stimulatory signals directly to T cells, as predicted by our logical simulations.

Discussion

We generated detailed molecular maps and logical models for TCR and TLR5 signaling pathways, which were adapted to human naïve $CD4^+$ T cells, taking into account the expression and epigenetic status of the main genes involved. These models were fine-tuned until reaching a behavior in agreement with experimental data, including four documented perturbations. These models were then merged to generate a combined "TCR + TLR5" model, which was used to predict the activation of key transcription factors upon induction of each or both pathways. Simulation results were compared with experimental results regarding the activation of c-Jun (AP-1), CREB, and p65 (NF-κB). Our simulations and experimental results point to a potential role of TLR5 co-stimulatory signals in the activation and differentiation of $CD4^+$ T cells through the induction of AP-1, CREB, and NF-κB activation, which can in turn induce (directly or through other transcription factors) the expression of several genes encoding cytokines, receptors, and signaling molecules.

According to our modeling and experimental results, the TLR5 pathway cooperates with TCR signals to induce NF-κB and AP-1 activation. This could explain the role of TLR5 in the proliferation of $CD4^+$ T cells, as well as the production of the cytokines IFN-γ and IL-8 (58). However, although both the TCR and TLR5 resulted in the activation of common transcription factors, the signaling pathways leading to transcription factor activation were mostly independent. This suggests that the TLR5 pathway could act as a rescue pathway to enable $CD4^+$ T cell activation in immunodeficient conditions, for example, when important signaling molecules of the TCR pathway are inactive or inadequately functioning. In this respect, we previously recently reported (78) that TLR5 signals play a proinflammatory role in neonatal and adult $CD4^+$ T cells,

leading to the production of IFN-γ. Thus, TLR5 contributes to overcome the higher activation threshold of neonatal $CD4^+$ T cells, which are characterized by defective TCR/CD28–mediated AP-1 activation (79). Consistent with this finding, flagellin is a good adjuvant, inducing protection in a neonatal mouse vaccination model of rotavirus infection (78).

In summary, combining computational modeling and experimental validations, our combined experimental and modeling analysis demonstrates that TLR5 is a co-stimulatory receptor for $CD4^+$ T cells, and that it uses a different pathway than that used by CD28 to induce the activation of the transcription factors NF-κB and AP-1. This function of TLR5 is independent of its role in innate immunity, because our experiments were performed with isolated, naive $CD4^+$ T cells. However, both functions of TLR5 might be important for a full immune response in vivo.

Materials and Methods

Generation of molecular maps

We generated detailed molecular maps for the TCR and TLR5 signaling pathways using the software CellDesigner (http://www.celldesigner.org/). To do this, we relied on data gathered from the literature and from databases such as KEGG (http://www.genome.jp/kegg/), Reactome (http://www.reactome.org/), and DC-ATLAS (http://compbiotoolbox.fmach.it/DCATLAS.php). In CellDesigner, there are three possible types of Components, which are Species, Reactions, and Compartments. A Species represents a protein, a complex, or some other molecule in a biochemical or regulatory network. On the other hand, a Reaction can be a chemical reaction, a physical interaction between Species, or a regulatory relation between genes. Finally, a Compartment represents a container for other components, such as a cell or an intracellular

compartment. All species and reactions of the molecular maps are annotated with textual comments and hyperlinks to record the supporting information and its source (see Files 1 and 3).

Generation of logical models

We built our logical models using the software GINsim (www.ginsim.org), relying on the molecular maps previously generated. GINsim implements the multivalued logical modeling formalism introduced by Thomas and D'Ari (80). This formalism relies on the delineation of a regulatory graph (LRG), where each component (protein or more abstract biological function) is represented by a logical node (taking the values 0 or 1, or additional values when justified), and each influence (activation or inhibition) between a pair of components is represented by a signed arc. Next, a logical rule is assigned to each node in the network, which determines its activation level according to the levels of its regulators. These logical rules involve literals (component values) and the logical operators AND, OR and NOT (81, 82). We confirmed the expression of all model components in unstimulated naïve $CD4^+$ T cells using RNA-seq and ChIP-seq data reported by the BLUEPRINT consortium (Table S1). A gene was considered expressed if it could be associated with regions with chromatin marks denoting active promoters or enhancers, together with an expression value of at least 1 RPKM (Reads Per Kilobase of transcripts, per Million mapped). ChIP-seq peaks of histone modifications were given as input to the software ChromHMM (http://compbio.mit.edu/ChromHMM/) (with the parameters BinerizeBed –center option, assembly hg38; LearnModel 10 states) to segment the genome in different regions according to their chromatin states. We then selected the regions associated with marks of active promoters ($H3K4me3^+H3K27ac^+$) and enhancers ($H3K4me1^+H3K27ac^+$).

Model analysis

The two original models for the TCR and TLR5 signaling pathways were merged and the logical rules of shared nodes were updated to take into account the additional regulatory inputs (Fig. 5, Table S4, and File 5). We computed the stable states of the two original and merged models under wild-type and mutant conditions. We further generated a reduced version of the merged model (Fig. S4) to explore its dynamical behavior. All of the analyses were performed with GINsim [as previously described (81–84)], which supports model reduction by hiding selected (intermediate) nodes. Provided that no functional regulatory circuit is eliminated in the process, this reduction preserves all attractors (81). The dynamical behavior of a logical model is represented by a State Transition Graph (STG). In this graph, each node represents a state of the model, which is defined by a vector encompassing the levels of all components, and the arcs represent transitions between states. One core function of GINsim is the automatic construction of this graph (82). When the number of components in a model is large, the resulting STG becomes difficult to compute and to visualize. In this respect, GINsim enables the generation of a Hierarchical Transition Graph (HTG), which is computed by clustering the nodes of a STG into groups of states (hyper-nodes) sharing the same set of successors (84). Finally, computing the HTG for different initial conditions enabled us to identify all of the attractors of our merged model for wild-type and mutant scenarios (see Results).

Cell isolation and culture

Leukocyte concentrates were obtained from healthy donors from the “Centro Estatal de la Transfusión Sanguínea”, Cuernavaca, Mexico. Peripheral blood mononuclear cells (PBMCs) were obtained from these cellular concentrates through centrifugation with ficoll-hypaque gradient.

Total $CD4^+$ T cells were obtained using the RosetteSep $CD4^+$ T cell enrichment cocktail (Stem Cell) and 1 ml of erythrocytes from the same donor. We depleted memory cells with an anti-CD45RO antibody (Tonbo) coupled to magnetic beads (Pierce) with the help of a magnetic rack. Naive $CD4^+$ T cells obtained this way were cultured in RPMI medium supplemented with 5% fetal bovine serum (FBS) at 37°C with 5% CO_2. Cell preparations were routinely checked for purity and were at least 96% $CD3^+CD4^+$, $CD45RO^-$, and 96% $CCR7^+CD62L^+$.

$CD4^+$ T cell stimulation

Naive $CD4^+$ T cells were either left unstimulated or stimulated by cross-linking the CD3 receptor (simulating TCR ligation), with flagellin (to activate TLR5), with both stimuli (TCR + TLR5 activation), or by cross-linking CD3 and CD28 (TCR + CD28 activation). The activation of the following molecules was evaluated by flow cytometry: p65 (pp65), CREB (pCREB), c-Jun (pc-Jun). Cells were stimulated in RPMI medium supplemented with 2% FBS. The following antibodies were used at 1 µg/ml and 0.1 µg/ml in different combinations: anti-CD3 (OKT3) (Tonbo) antibody, anti-CD28 (CD28.2) (Tonbo) antibody, and polyclonal goat anti-mouse antibody (Biolegend) to crosslink the anti-CD3 and anti-CD28 antibodies. TLR5 signals were induced with flagellin monomer (Invivogen) at final concentrations of 250 or 25 ng/ml.

Flow cytometry

To evaluate the purity of cell preparations, the following markers were evaluated by extracellular staining: CD3, CD4, CD45RO, CD45RA, CCR7, and CD62L. This consisted of the incubation of cells with antibody solutions for 30 min at 4°C, washing with PBS supplemented with 2% FBS, and a fixation step with 1% formaldehyde. The following antibodies were used: anti-CD3-PE

(Tonbo), anti-CD4-APC (Biolegend), anti-CD62L-PE (Miltenyi), anti-CCR7-FITC (Miltenyi), anti-CD45RO-FITC (Tonbo), and anti-CD45RA-FITC (Miltenyi). The activation of p65, CREB, and c-Jun was evaluated by intracellular staining. This consisted of the fixation of cells with 1.5% formaldehyde for 10 min, a permeabilization step with cold absolute MeOH for 10 min (0°C) or more (-80°C), a washing step with PBS supplemented with 2% FBS, incubation with antibody solution for 30 min at 4°C, and another washing step together with a final fixation step with 1% formaldehyde Activations of p65, c-Jun and CREB were evaluated by flow cytometry. Activation was determined by evaluating the phosphorylated protein in specific reported residues. We used anti-pc-Jun (Ser^{63}) (Genetex), anti-pCREB (Ser^{133}) (Pierce), a secondary anti-rabbit-FITC (Genetex) and anti-pp65 (Ser^{529})-APC (Miltenyi Biotec) antibodies. A FACScanto II (BD Biosciences) cytometer was used and data analysis was performed using the FlowJo software (Tree Star Ca). Changes of activated protein levels across pairs of conditions were assessed using Kruskal-Wallis tests and the software GrahPad Prism 7 (Tables S6, S7 and S8).

Supplementary Materials

File 1. TCR molecular map (to open with the software CellDesigner).
File 2. TCR signaling model (to open with the software GINsim).
File 3. TLR5 molecular map (to open with the software CellDesigner).
File 4. TLR5 signaling model (to open with the software GINsim).
File 5. TCR+TLR5 merged model (to open with the software GINsim).

References and Notes

1. Jenkins, M. K., a Khoruts, E. Ingulli, D. L. Mueller, S. J. McSorley, R. L. Reinhardt, a Itano, and K. a Pape. 2001. In vivo activation of antigen-specific CD4 T cells. *Annu. Rev. Immunol.* 19: 23–45.
2. Itano, A. A., and M. K. Jenkins. 2003. Antigen presentation to naive CD4 T cells in the lymph node. *Nat Immunol* 4: 733–739.
3. Blum, J. S., P. a Wearsch, and P. Cresswell. 2013. Pathways of antigen processing. *Annu. Rev. Immunol.* 31: 443–473.
4. Yamamoto, T., M. Hattori, and T. Yoshida. 2007. Induction of T-cell activation or anergy determined by the combination of intensity and duration of T-cell receptor stimulation, and sequential induction in an individual cell. *Immunology* 121: 383–391.
5. Acuto, O., and F. Michel. 2003. CD28-mediated co-stimulation: a quantitative support for TCR signalling. *Nat. Rev. Immunol.* 3: 939–951.
6. Riha, P., and C. E. Rudd. 2010. CD28 co-signaling in the adaptive immune response. *Self. Nonself.* 1: 231–240.
7. Chen, L., and D. B. Flies. 2013. Molecular mechanisms of T cell co-stimulation and co-inhibition. *Nat. Rev. Immunol.* 13: 227–242.
8. Huang, Y., and R. L. Wange. 2004. T cell receptor signaling: beyond complex complexes. *J. Biol. Chem.* 279: 28827–28830.
9. Salmond, R. J., A. Filby, I. Qureshi, S. Caserta, and R. Zamoyska. 2009. T-cell receptor proximal signaling via the Src-family kinases, Lck and Fyn, influences T-cell activation, differentiation, and tolerance. *Immunol. Rev.* 228: 9–22.
10. Zehn, D., C. King, M. J. Bevan, and E. Palmer. 2012. TCR signaling requirements for activating T cells and for generating memory. *Cell. Mol. Life Sci.* 69: 1565–1575.
11. Poltorak, M., B. Arndt, B. B. S. Kowtharapu, A. V Reddycherla, V. Witte, J. A. J. Lindquist, B. Schraven, L. Simeoni, B. Kholodenko, C. Marshall, S. Santos, P. Verveer, P. Bastiaens, L. Murphy, S. Smith, R. Chen, D. Fingar, J. Blenis, M. Daniels, E. Teixeiro, J. Gill, B. Hausmann, D. Roubaty, K. Holmberg, G. Werlen, G. Hollander, N. Gascoigne, E. Palmer, X. Wang, L. Simeoni, J. A. J. Lindquist, J. Saez-Rodriguez, A. Ambach, E. Gilles, S. Kliche, B. Schraven, B. Arndt, M. Poltorak, B. B. S. Kowtharapu, P. Reichardt, L. Philipsen, J. A. J. Lindquist, B. Schraven, L. Simeoni, T. Brdicka, D. Pavlistova, A. Leo, E. Bruyns, V. Korinek, P. Angelisova, J. Scherer, A. Shevchenko, I. Hilgert, J. Cerny, N. Berg, L. Puente, W. Dawicki, H. Ostergaard, I. Stefanova, B. Hemmer, M. Vergelli, R. Martin, W. Biddison, R. Germain, G. Altan-Bonnet, R. Germain, O. Acuto, V. Di Bartolo, F. Micheli, S. Loeser, J. Penninger, S. Dong, B. Corre, E. Foulon, E. Dufour, A. Veillette, O. Acuto, F. Michel, G. Levkowitz, H. Waterman, S. Ettenberg, M. Katz, A. Tsygankov, I. Alroy, S. Lavi, K. Iwai, Y. Reiss, A. Ciechanover, C. Kassenbrock, S. Anderson, H. Wang, Y. Altman, D. Fang, C. Elly, Y. Dai, Y. Shao, Y. Liu, J. Watts, J. Sanghera, S. Pelech, R. Aebersold, D. Winkler, I. Park, T. Kim, N. Payne, C. Walsh, J. Strominger, J. Shin, I. Joung, T. Kim, L. Stolz, G. Payne, D. Winkler, C. Walsh, J. Strominger, J. Shin, T. Methi, T. Berge, K. Torgersen, K. Tasken, T. Methi, J. Ngai, M. Mahic, M. Amarzguioui, T. Vang, K.

Tasken, J. Neilson, M. Winslow, E. Hur, G. Crabtree, K. Nika, C. Soldani, M. Salek, W. Paster, A. Gray, R. Etzensperger, L. Fugger, P. Polzella, V. Cerundolo, O. Dushek, I. Bank, L. Chess, N. Banda, J. Bernier, D. Kurahara, R. Kurrle, N. Haigwood, R. Sekaly, T. Finkel, L. Puente, J. He, H. Ostergaard, B. Arndt, T. Krieger, T. Kalinski, A. Thielitz, D. Reinhold, A. Roessner, B. Schraven, and L. Simeoni. 2013. TCR activation kinetics and feedback regulation in primary human T cells. *Cell Commun. Signal.* 11: 4–14.
12. Mayya, V., D. H. Lundgren, S.-I. Hwang, K. Rezaul, L. Wu, J. K. Eng, V. Rodionov, and D. K. Han. 2009. Quantitative Phosphoproteomic Analysis of T Cell Receptor Signaling Reveals System-Wide Modulation of Protein-Protein Interactions. *Sci. Signal.* 2: ra46.
13. De Wet, B., T. Zech, M. Salek, O. Acuto, and T. Harder. 2011. Proteomic characterization of plasma membrane-proximal T cell activation responses. *J. Biol. Chem.* 286: 4072–4080.
14. Brockmeyer, C., W. Paster, D. Pepper, C. P. Tan, D. C. Trudgian, S. McGowan, G. Fu, N. R. J. J. Gascoigne, O. Acuto, and M. Salek. 2011. T cell receptor (TCR)-induced tyrosine phosphorylation dynamics identifies THEMIS as a new TCR signalosome component. *J. Biol. Chem.* 286: 7535–7547.
15. Salek, M., S. McGowan, D. C. Trudgian, O. Dushek, B. de Wet, G. Efstathiou, and O. Acuto. 2013. Quantitative phosphoproteome analysis unveils LAT as a modulator of CD3ζ and ZAP-70 tyrosine phosphorylation. *PLoS One* 8: e77423.
16. Roncagalli, R., S. Hauri, F. Fiore, Y. Liang, Z. Chen, A. Sansoni, K. Kanduri, R. Joly, A. Malzac, H. Lähdesmäki, R. Lahesmaa, S. Yamasaki, T. Saito, M. Malissen, R. Aebersold, M. Gstaiger, and B. Malissen. 2014. Quantitative proteomics analysis of signalosome dynamics in primary T cells identifies the surface receptor CD6 as a Lat adaptor-independent TCR signaling hub. *Nat. Immunol.* 15: 384–392.
17. Chylek, L. A., V. Akimov, J. Dengjel, K. T. G. Rigbolt, B. Hu, W. S. Hlavacek, and B. Blagoev. 2014. Phosphorylation site dynamics of early T-cell receptor signaling. *PLoS One* 9: e104240.
18. Malissen, B., C. Grégoire, M. Malissen, and R. Roncagalli. 2014. Integrative biology of T cell activation. *Nat. Immunol.* 15: 790–797.
19. Morris, G. P., and P. M. Allen. 2012. How the TCR balances sensitivity and specificity for the recognition of self and pathogens. *Nat. Immunol.* 13: 121–128.
20. Brownlie, R. J., and R. Zamoyska. 2013. T cell receptor signalling networks: branched, diversified and bounded. *Nat. Rev. Immunol.* 13: 257–269.
21. Paul, S., and B. C. Schaefer. 2013. A new look at T cell receptor signaling to nuclear factor-κB. *Trends Immunol.* 34: 269–281.
22. Thaker, Y. R., H. Schneider, and C. E. Rudd. 2014. TCR and CD28 activate the transcription factor NF-κB in T-cells via distinct adaptor signaling complexes. *Immunol. Lett.* 163: 113–119.
23. Coudronniere, N., M. Villalba, N. Englund, and A. Altman. 2000. NF-kappa B activation induced by T cell receptor/CD28 costimulation is mediated by protein kinase C-theta. *Proc. Natl. Acad. Sci. U. S. A.* 97: 3394–3399.
24. Michel, F., G. Attal-Bonnefoy, G. Mangino, S. Mise-Omata, and O. Acuto. 2001. CD28 as a molecular amplifier extending TCR ligation and signaling capabilities. *Immunity* 15: 935–945.
25. Yeh, J., P. Lecine, J. a Nunes, S. Spicuglia, P. Ferrier, D. Olive, and J. Imbert. 2001. Novel CD28-Responsive Enhancer Activated by CREB / ATF and AP-1 Families in the Human Interleukin-2 Receptor α-Chain Locus. *Mol. Cell. Biol.* 21: 4515–4527.
26. Liberman, A. C., D. Refojo, and E. Arzt. 2003. Cytokine signaling/transcription factor cross-talk in T cell activation and Th1-Th2 differentiation. *Arch. Immunol. Ther. Exp. (Warsz).* 51: 351–

365.
27. Kaiser, M., G. R. Wiggin, K. Lightfoot, S. S. C. Arthur, and A. Macdonald. 2007. MSK regulate TCR-induced CREB phosphorylation but not immediate early gene transcription. *Eur. J. Immunol.* 37: 2583–2595.
28. Wen, A. Y., K. M. Sakamoto, and L. S. Miller. 2010. The Role of the Transcription Factor CREB in Immune Function. *J. Immunol.* 185: 6413–6419.
29. Sundstedt, A., M. Sigvardsson, T. Leanderson, G. Hedlund, T. Kalland, and M. Dohlsten. 1996. In vivo anergized CD4+ T cells express perturbed AP-1 and NF-kappa B transcription factors. *Proc. Natl. Acad. Sci. U. S. A.* 93: 979–984.
30. Clavijo, P. E., Frauwirth, K. A., P. E. Clavijo, K. a. Frauwirth, and K. A. Clavijo, P. E., Frauwirth. 2012. Anergic CD8+ T Lymphocytes Have Impaired NF- B Activation with Defects in p65 Phosphorylation and Acetylation. *J. Immunol.* 188: 1213–1221.
31. Müller, M. R., and A. Rao. 2010. NFAT, immunity and cancer: a transcription factor comes of age. *Nat. Rev. Immunol.* 10: 645–656.
32. Serfling, E., F. Berberich-Siebelt, A. Avots, S. Chuvpilo, S. Klein-Hessling, M. K. Jha, E. Kondo, P. Pagel, J. Schulze-Luehrmann, and A. Palmetshofer. 2004. NFAT and NF-κB factors - The distant relatives. *Int. J. Biochem. Cell Biol.* 36: 1166–1170.
33. Oh, H., and S. Ghosh. 2013. NF-κB: roles and regulation in different CD4(+) T-cell subsets. *Immunol. Rev.* 252: 41–51.
34. Hermann-Kleiter, N., and G. Baier. 2010. NFAT pulls the strings during CD4+ T helper cell effector functions. *Blood* 115: 2989–2997.
35. Baine, I., B. T. Abe, and F. Macian. 2009. Regulation of T-cell tolerance by calcium/NFAT signaling. *Immunol. Rev.* 231: 225–240.
36. Lin, L., M. Spoor, A. Gerth, S. Brody, and S. Peng. 2004. Modulation of Th1 Activation and Inflammation by the NF- κB Repressor Foxj1. *Science.* 303: 1017–1020.
37. Lovatt, M., and M. J. Bijlmakers. 2010. Stabilisation of β-catenin downstream of T cell receptor signalling. *PLoS One* 5: 1–8.
38. Driessens, G., Y. Zheng, F. Locke, J. L. Cannon, F. Gounari, and T. F. Gajewski. 2011. Beta-catenin inhibits T cell activation by selective interference with linker for activation of T cells-phospholipase C-γ1 phosphorylation. *J. Immunol.* 186: 784–90.
39. Charvet, C., P. Auberger, S. Tartare-Deckert, A. Bernard, and M. Deckert. 2002. Vav1 couples T cell receptor to serum response factor-dependent transcription via a MEK-dependent pathway. *J. Biol. Chem.* 277: 15376–15384.
40. Crellin, N. K., R. V Garcia, O. Hadisfar, S. E. Allan, T. S. Steiner, and M. K. Levings. 2005. Human CD4+ T cells express TLR5 and its ligand flagellin enhances the suppressive capacity and expression of FOXP3 in CD4+CD25+ T regulatory cells. *J. Immunol.* 175: 8051–8059.
41. Tremblay, M. M., M. Y. Bilal, and J. C. D. Houtman. 2014. Prior TLR5 induction in human T cells results in a transient potentiation of subsequent TCR-induced cytokine production. *Mol. Immunol.* 57: 161–170.
42. Kollmann, T. R., O. Levy, R. R. Montgomery, and S. Goriely. 2012. Innate immune function by Toll-like receptors: distinct responses in newborns and the elderly. *Immunity* 37: 771–83.
43. Medzhitov, R. 2001. Toll-like receptors and innate immunity. *Nat. Rev. Immunol.* 1: 135–145.
44. Takeda, K., and S. Akira. 2005. Toll-like receptors in innate immunity. *Int. Immunol.* 17: 1–14.
45. Takeda, K., and S. Akira. 2004. TLR signaling pathways. *Semin. Immunol.* 16: 3–9.
46. Akira, S. 2003. Toll-like receptor signaling. *J. Biol. Chem.* 278: 38105–38108.

47. Lim, K.-H., and L. M. Staudt. 2013. Toll-like receptor signaling. *Cold Spring Harb. Perspect. Biol.* 5: a011247.
48. Kawasaki, T., and T. Kawai. 2014. Toll-like receptor signaling pathways. *Front. Immunol.* 5: 1–8.
49. Li, X., S. Jiang, and R. I. Tapping. 2010. Toll-like receptor signaling in cell proliferation and survival. *Cytokine* 49: 1–9.
50. Brown, J., H. Wang, G. N. Hajishengallis, and M. Martin. 2011. TLR-signaling networks: an integration of adaptor molecules, kinases, and cross-talk. *J. Dent. Res.* 90: 417–427.
51. Troutman, T. D., J. F. Bazan, and C. Pasare. 2012. Toll-like receptors, signaling adapters and regulation of the pro-inflammatory response by PI3K. *Cell Cycle* 11: 3559–3567.
52. Taniguchi, K. H. and T. 2006. IRFs : master regulators of signalling by Toll-like receptors and cytosolic pattern-recognition receptors. *Nat. Rev. Immunol.* 6: 644–658.
53. Honda, K., and T. Taniguchi. 2006. Toll-like receptor signaling and IRF transcription factors. *IUBMB Life* 58: 290–295.
54. Mori, J., T. Vranac, B. Smrekar, M. Cernilec, V. Č. Serbec, S. Horvat, A. Ihan, M. Benčina, and R. Jerala. 2012. Chimeric flagellin as the self-adjuvanting antigen for the activation of immune response against Helicobacter pylori. *Vaccine* 30: 5856–5863.
55. Kim, J. R., B. C. Holbrook, S. L. Hayward, L. K. Blevins, M. J. Jorgensen, N. D. Kock, K. De Paris, R. B. J. D'Agostino, S. T. Aycock, S. B. Mizel, G. D. Parks, and M. A. Alexander-Miller. 2015. Inclusion of Flagellin during Vaccination against Influenza Enhances Recall Responses in Nonhuman Primate Neonates. *J. Virol.* 89: 7291–7303.
56. Salman, H. H., J. M. Irache, and C. Gamazo. 2009. Immunoadjuvant capacity of flagellin and mannosamine-coated poly(anhydride) nanoparticles in oral vaccination. *Vaccine* 27: 4784–4790.
57. Mizel, S. B., and J. T. Bates. 2010. Flagellin as an adjuvant: cellular mechanisms and potential. *J. Immunol.* 185: 5677–5682.
58. Caron, G., D. Duluc, I. Fremaux, P. Jeannin, C. David, H. Gascan, and Y. Delneste. 2005. Direct Stimulation of Human T Cells via TLR5 and TLR7/8: Flagellin and R-848 Up-Regulate Proliferation and IFN- Production by Memory CD4+ T Cells. *J. Immunol.* 175: 1551–1557.
59. Gibbons, D., P. Fleming, A. Virasami, M.-L. Michel, N. J. Sebire, K. Costeloe, R. Carr, N. Klein, and A. Hayday. 2014. Interleukin-8 (CXCL8) production is a signatory T cell effector function of human newborn infants. *Nat. Med.* 20: 1206–1210.
60. McCarron, M., and D. J. Reen. 2009. Activated human neonatal CD8+ T cells are subject to immunomodulation by direct TLR2 or TLR5 stimulation. *J. Immunol.* 182: 55–62.
61. Saez-Rodriguez, J., L. Simeoni, J. a Lindquist, R. Hemenway, U. Bommhardt, B. Arndt, U.-U. Haus, R. Weismantel, E. D. Gilles, S. Klamt, and B. Schraven. 2007. A logical model provides insights into T cell receptor signaling. *PLoS Comput. Biol.* 3: e163.
62. Bai, D., L. Ueno, and P. Vogt. 2009. Akt-mediated regulation of NFkB and the essentialness of NFkB for the oncogenicity of PI3K and Akt. *Int J Cancer* 125: 2863–2870.
63. Chiu, Y.-C., C.-Y. Lin, C.-P. Chen, K.-C. Huang, K.-M. Tong, C.-Y. Tzeng, T.-S. Lee, H.-C. Hsu, and C.-H. Tang. 2009. Peptidoglycan Enhances IL-6 Production in Human Synovial Fibroblasts via TLR2 Receptor, Focal Adhesion Kinase, Akt, and AP-1- Dependent Pathway. *J. Immunol.* 183: 2785–2792.
64. Sun, Z., C. W. Arendt, W. Ellmeier, E. M. Schaeffer, M. J. Sunshine, L. Gandhi, J. Annes, D. Petrzilka, a Kupfer, P. L. Schwartzberg, and D. R. Littman. 2000. PKC-theta is required for TCR-induced NF-kappaB activation in mature but not immature T lymphocytes. *Nature* 404: 402–407.
65. Wuerzberger-Davis, S. M., and S. Miyamoto. 2010. TAK-ling IKK activation: "Ub" the judge.

Sci. Signal. 3: pe3.
66. Adhikari, A., M. Xu, and Z. J. Chen. 2007. Ubiquitin-mediated activation of TAK1 and IKK. *Oncogene* 26: 3214–3226.
67. Fan, Y., Y. Yu, Y. Shi, W. Sun, M. Xie, N. Ge, R. Mao, A. Chang, G. Xu, M. D. Schneider, H. Zhang, S. Fu, J. Qin, and J. Yang. 2010. Lysine 63-linked polyubiquitination of TAK1 at lysine 158 is required for tumor necrosis factor alpha- and interleukin-1beta-induced IKK/NF-kappaB and JNK/AP-1 activation. *J. Biol. Chem.* 285: 5347–5360.
68. Mellett, M., P. Atzei, R. Jackson, L. a O'Neill, and P. N. Moynagh. 2011. Mal mediates TLR-induced activation of CREB and expression of IL-10. *J. Immunol.* 186: 4925–4935.
69. Hazeki, K., K. Nigorikawa, and O. Hazeki. 2007. Role of phosphoinositide 3-kinase in innate immunity. *Biol. Pharm. Bull.* 30: 1617–1623.
70. Martin, M., K. Rehani, R. S. Jope, and S. M. Michalek. 2005. Toll-like receptor-mediated cytokine production is differentially regulated by glycogen synthase kinase 3. *Nat. Immunol.* 6: 777–784.
71. Härtel, C., G. Bein, H. Kirchner, and H. Klüter. 1999. A human whole-blood assay for analysis of T-cell function by quantification of cytokine mRNA. *Scand. J. Immunol.* 49: 649–654.
72. Elly, C., S. Witte, Z. Zhang, O. Rosnet, S. Lipkowitz, A. Altman, and Y. C. Liu. 1999. Tyrosine phosphorylation and complex formation of Cbl-b upon T cell receptor stimulation. *Oncogene* 18: 1147–1156.
73. Appleman, L. J., A. a F. L. van Puijenbroek, K. M. Shu, L. M. Nadler, and V. a Boussiotis. 2002. CD28 costimulation mediates down-regulation of p27kip1 and cell cycle progression by activation of the PI3K/PKB signaling pathway in primary human T cells. *J. Immunol.* 168: 2729–2736.
74. Holzer, U., W. W. Kwok, G. T. Nepom, and J. H. Buckner. 2003. Differential antigen sensitivity and costimulatory requirements in human Th1 and Th2 antigen-specific CD4+ cells with similar TCR avidity. *J. Immunol.* 170: 1218–1223.
75. Schmiedeberg, K., H. Krause, F. W. RÖhl, R. Hartig, G. Jorch, and M. C. Brunner-Weinzierl. 2016. T cells of infants are mature, but hyporeactive due to limited Ca2+influx. *PLoS One* 11: 1–27.
76. Borovsky, Z., G. Mishan-eisenberg, E. Yaniv, and J. Rachmilewitz. 2002. Serial Triggering of T Cell Receptors Results in Incremental Accumulation of Signaling Intermediates *. 277: 21529–21536.
77. Zhang, J., T. Bardos, D. Li, I. Gal, C. Vermes, J. Xu, K. Mikecz, A. Finnegan, S. Lipkowitz, and T. T. Glant. 2002. Cutting Edge: Regulation of T Cell Activation Threshold by CD28 Costimulation Through Targeting Cbl-b for Ubiquitination. *J. Immunol.* 169: 2236–2240.
78. Labastida-conde, R. G., O. Ramírez-pliego, M. Peleteiro-olmedo, D. V. Lopez-guerrero, O. D. Badillo-Godinez, M. de L. Gutiérrez-xicoténcatl, G. Rosas-salgado, Á. González-fernández, F. R. Esquivel-guadarrama, and M. A. Santana. 2018. Flagellin is a Th1 polarizing factor for human CD4 + T cells and induces protection in a murine neonatal vaccination model of rotavirus infection. *Vaccine* 36: 1–10.
79. Palin, A. C., V. Ramachandran, S. Acharya, and D. B. Lewis. 2013. Human neonatal naive CD4+ T cells have enhanced activation-dependent signaling regulated by the microRNA miR-181a. *J. Immunol.* 190: 2682–91.
80. Thomas, R., and R. D'Ari. 1990. *Biological feedback*,. CRC Press, Inc.
81. Grieco, L., L. Calzone, I. Bernard-pierrot, B. Kahn-perle, F. Radvanyi, B. Kahn-Perlès, D. Thieffry, and B. Kahn-perle. 2013. Integrative Modelling of the Influence of MAPK Network on

Cancer Cell Fate Decision. *PLoS Comput. Biol.* 9: e1003286.
82. Naldi, A., C. Hernandez, W. Abou-Jaoudé, P. T. Monteiro, C. Chaouiya, and D. Thieffry. 2018. Logical modelling and analysis of cellular regulatory networks with GINsim 3.0. *Front. Physiol.* 9: 289–298.
83. Collombet, S., C. van Oevelen, J. L. Sardina Ortega, W. Abou-Jaoudé, B. Di Stefano, M. Thomas-Chollier, T. Graf, and D. Thieffry. 2017. Logical modeling of lymphoid and myeloid cell specification and transdifferentiation. *Proc. Natl. Acad. Sci.* 114: 5792–5799.
84. Bérenguier, D., C. Chaouiya, P. T. Monteiro, A. Naldi, E. Remy, D. Thieffry, and L. Tichit. 2013. Dynamical modeling and analysis of large cellular regulatory networks. *Chaos* 23: 0251141–0251149.

Acknowledgments: We thank the members of the Thieffry and Santana teams for their advice on the presentation of this manuscript and many insightful discussions. We further thank Erika I. Melchy and Carlos Mojica for their assistance with flow cytometry. **Funding**: O. RJ was awarded a doctoral scholarship from Consejo Nacional de Ciencia y Tecnología (CONACYT) (253310). The A.S. laboratory is supported by grants from CONACYT (168182 and 257188) and Programa de Mejoramiento del Profesorado (PROMEPSI- UAEM/13/342). The D.T. laboratory has been supported by grants from the French Plan Cancer, in the context of the projects CoMET (2014–2017) and SYSTAIM (2015-2019), as well as by a grant from the French Agence Nationale pour la Recherche, in the context of the project TMod (2016-2020). This project also received funding from SEP-CONACYT-ANUIES-ECOS NORD (M11S01 and M17S02). **Author contributions**: O. R-J generated and validated the logical models under the supervision of D. T. and performed the experiments under the supervision of A. S. L. A. K. purified cells and performed experiments. W. A. generated the TLR5 molecular map and contributed to the analyses performed with GINsim. D. Y. G. purified cells. C. H. generated the TCR molecular map. O. R-P. assisted in the technical details of cell purification and culture. M. T-C. and S. S contributed to the NGS data analyses. A. S., O. R-J and D. T. conceived and wrote the manuscript, whereas all authors endorse its content. **Competing interests**: The authors declare that they have no competing interests. **Data and materials availability**: All RNA-seq and ChIP-seq data used here was published by the BLUEPRINT consortium (see Table S1). Furthermore, the TCR, TLR5 and merged Boolean models are available in GINsim format in the GINsim model repository (http://ginsim.org/node/225), as well as in SBML-qual format in the BioModels database (ID: MODEL1903260001, MODEL1903260002, MODEL1903260003). . All data needed to evaluate the conclusions in the paper are present in the paper or the Supplementary Materials.

Figures.

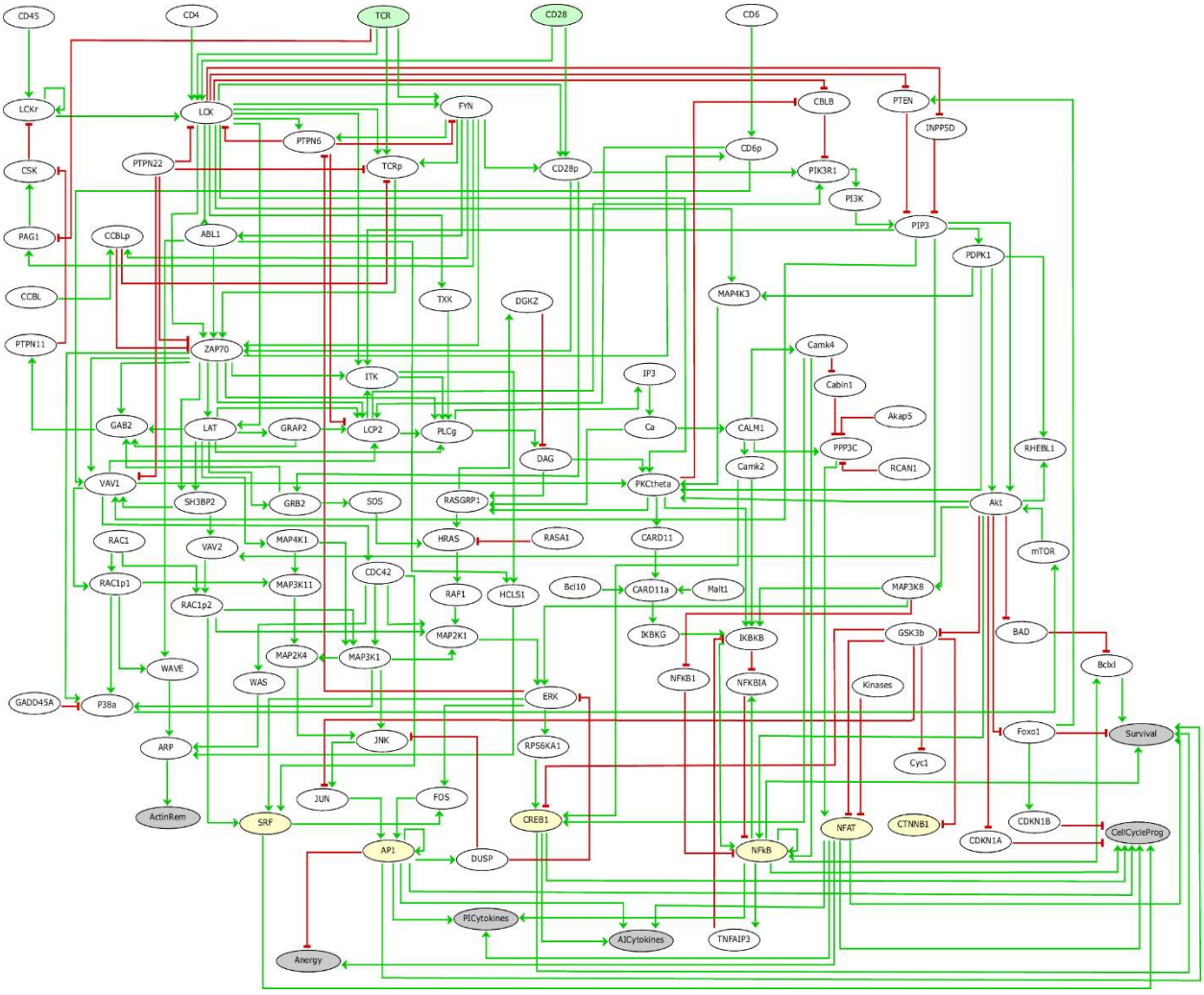

Fig. 1. The TCR signaling model. The model encompasses 110 nodes, including two externally controlled inputs (TCR and CD28), which are depicted in green, six activated transcription factors, which are in yellow, and six phenotypical outputs, which are in gray. Green arrows represent activation events, whereas red blunt-end arcs denote inhibition events. PICytokines, proinflammatory cytokines; AICytokines, anti-inflammatory cytokines.

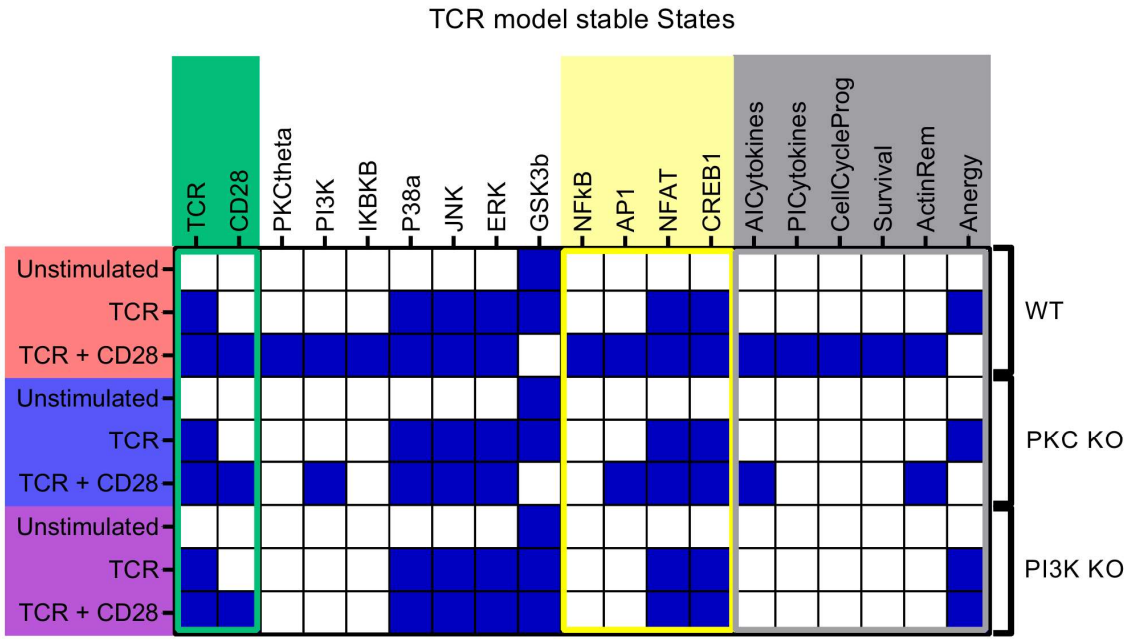

Fig. 2. Computation of the stable states of the TCR model. The rows list the stable states identified with GINsim software for three distinct scenarios [Wild-type (WT), PKCθ KO, and PI3K KO) and three environmental conditions (Unstimulated, TCR stimulation, or TCR + CD28 stimulation). Note that only the relevant nodes are displayed. White cells (zero value) denote negligible activation of the corresponding components (columns), whereas blue cells (value of 1) denote substantial activation. Inputs are highlighted in green, phenotypical nodes are in gray, and the transcription factors induced during T cell activation are in yellow. CellCycleProg, cell cycle progression; ActinRem, actin remodeling.

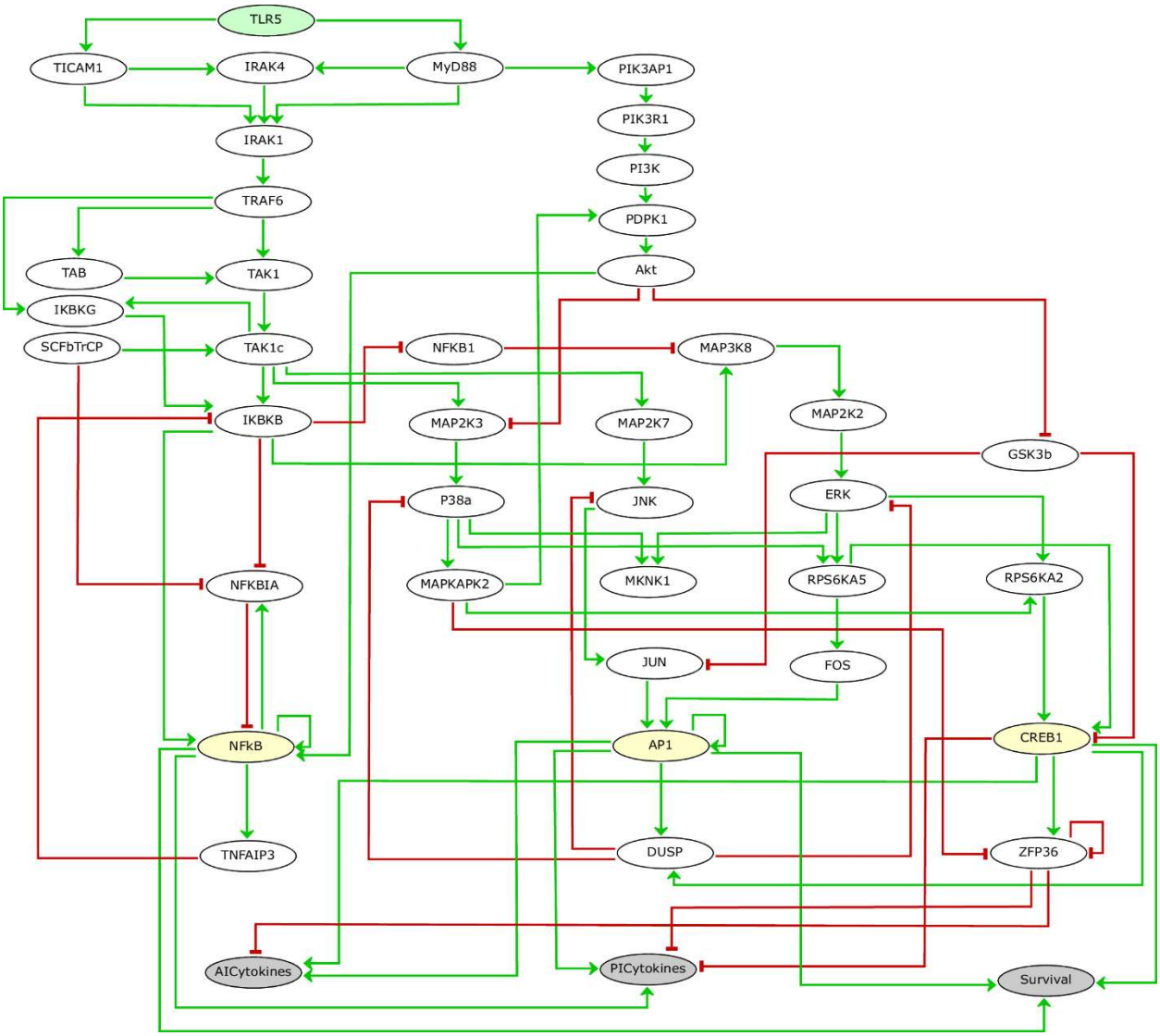

Fig. 3. The TLR5 signaling model. The model encompasses 42 nodes, among which one corresponds to the TLR5 input (green), three correspond to key three transcription factors (yellow), and three to phenotypical output nodes (gray). Green arrows represent activation events, whereas red blunt-end arcs denote inhibition events.

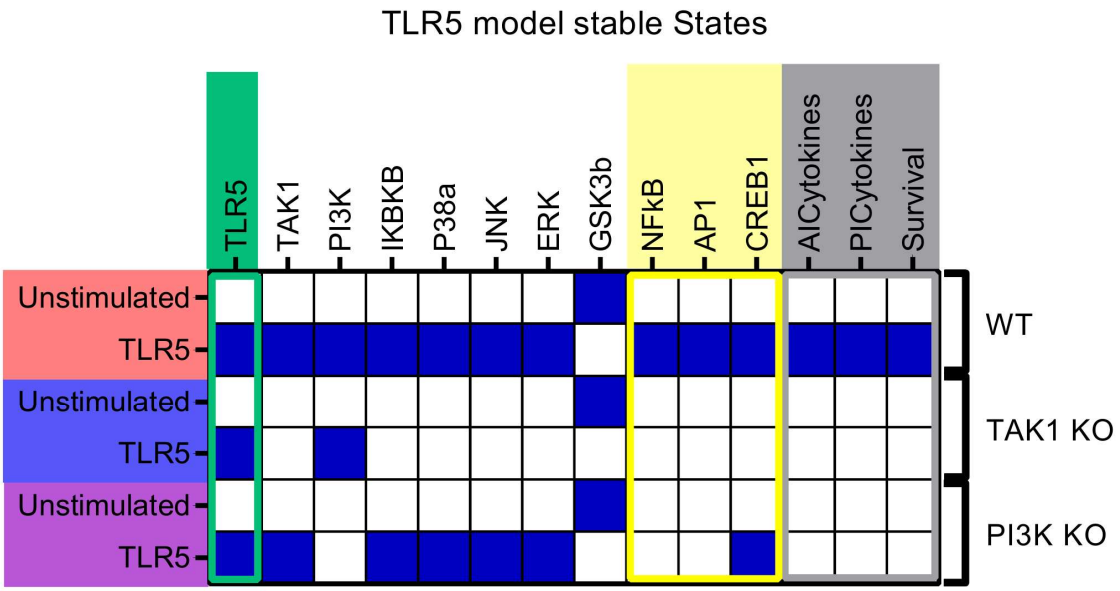

Fig. 4. Computation of the stable states of the TLR5 model. The rows list the stable states identified for three distinct scenarios [Wild-type (WT), TAK1 KO, and PI3K KO] and two environmental conditions (Unstimulated, TLR5 stimulation). White cells (value 0) denote negligible activation of the corresponding components (columns), whereas blue cells (value 1) denote substantial activation. Inputs are highlighted in green, phenotypical nodes are in gray, and the transcription factors induced during T cell activation are in yellow.

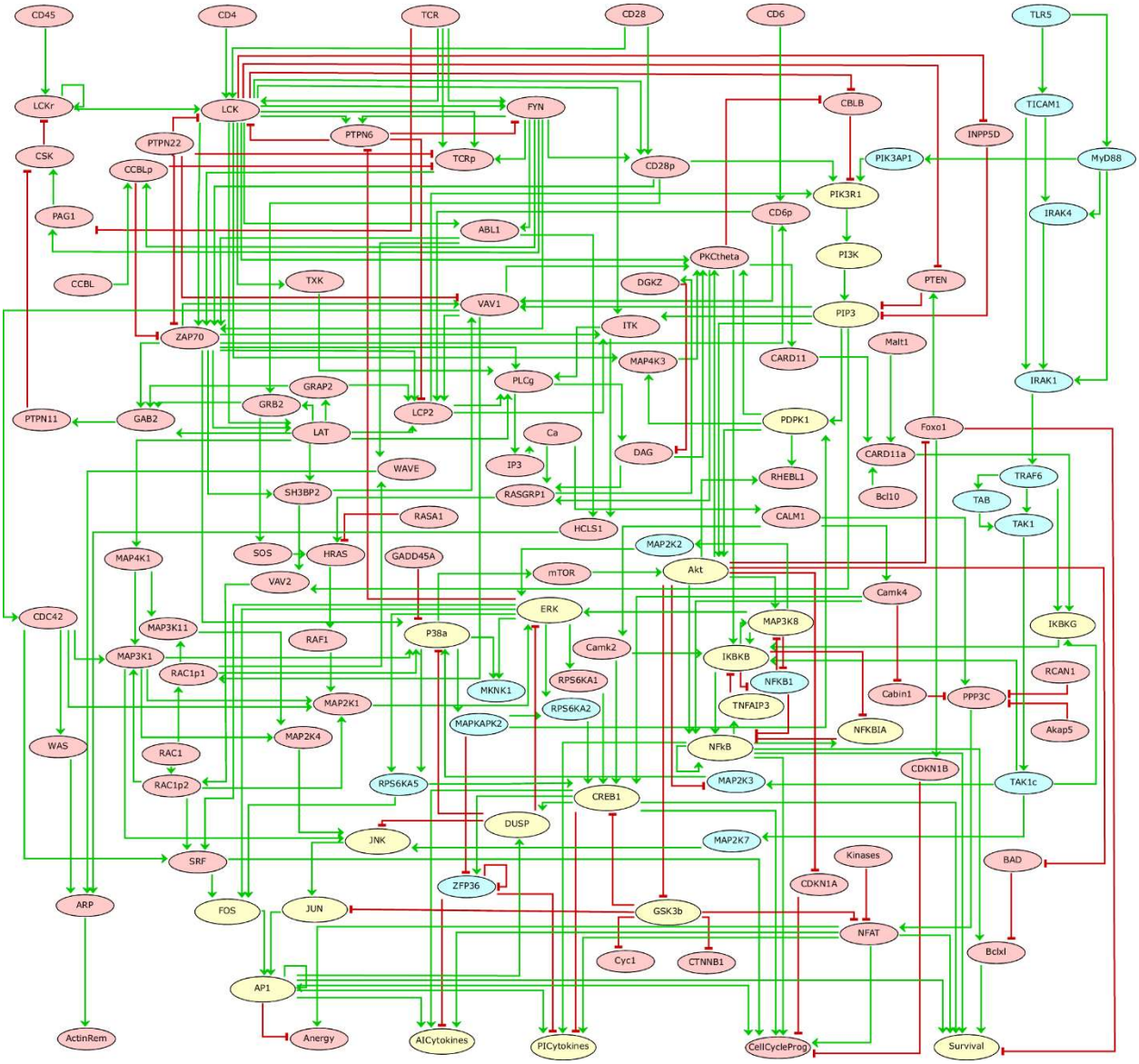

Fig. 5. The TCR+TLR5 merged model. The merged model encompasses 128 nodes, including three externally controlled inputs (TLR5, TCR, and CD28) and six phenotypic nodes (bottom). The pink nodes belong to the original TCR model, the blue nodes belong exclusively to the original TLR5 model, and the yellow nodes are shared between the two models. Green arrows represent activation events, whereas red, blunt-end arcs denote inhibition events.

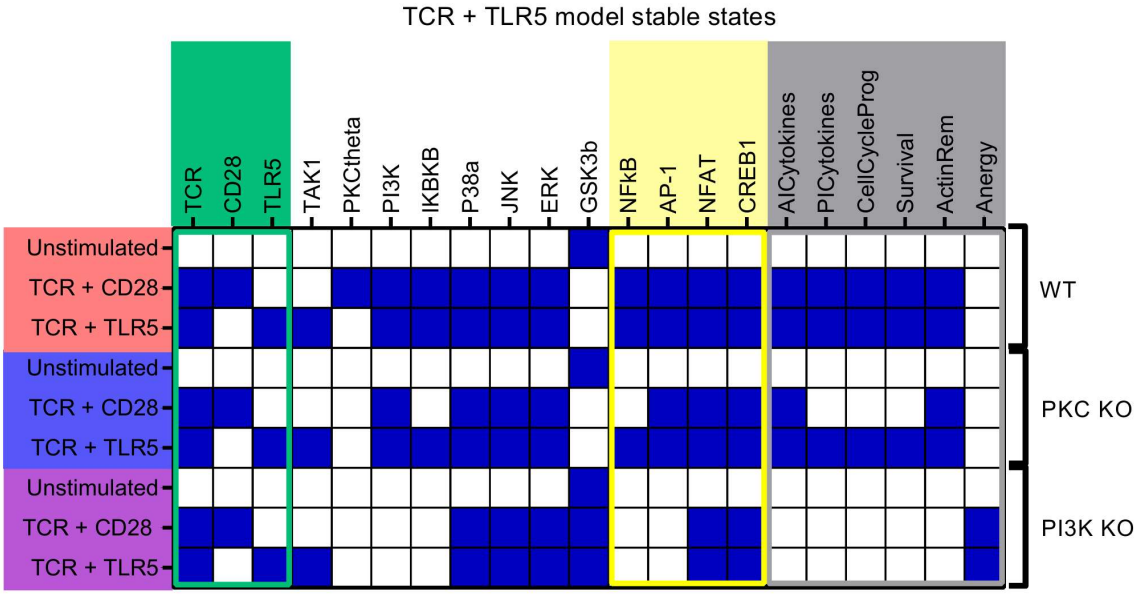

Fig. 6. Computation of the stable states for the TCR + TLR5 merged model. The rows list the stable states identified for three distinct scenarios [Wild-type (WT), PKCθ KO, and PI3K KO) and three environmental conditions (Unstimulated, TCR + CD28 stimulation, and TCR + TLR5 stimulation). White cells (value 0) denote negligible activation of the corresponding components (columns), whereas blue cells (value 1) denote substantial activation. Inputs are highlighted in green, phenotypical nodes are in grzy, and the transcription factors induced during T cell activation are in yellow.

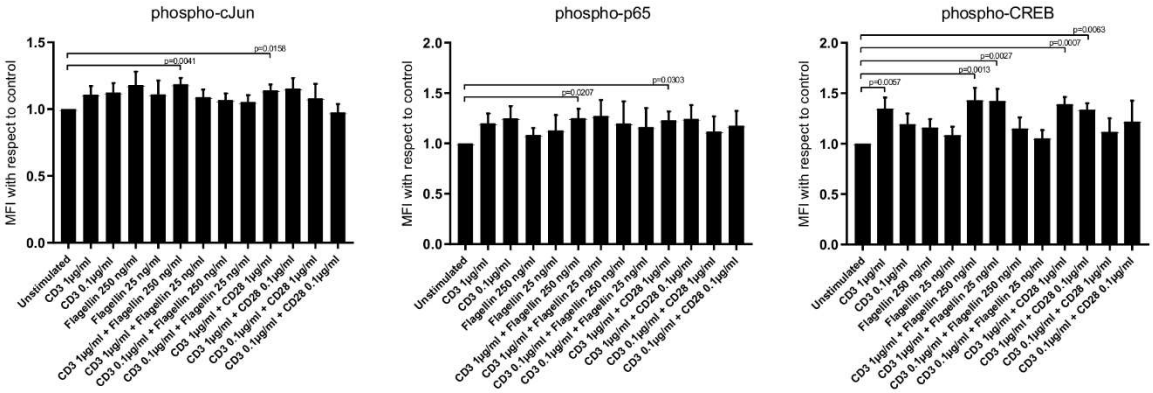

Fig. 7. Experimental assessment of AP-1, NF-κB, and CREB activities. We used flow cytometry to evaluate the phosphorylation of c-Jun, p65, and CREB1, as a measure of the activation of AP-1, NF-κB, and CREB, respectively. Naive CD4+ T cells were left unstimulated or were stimulated under the indicated conditions for 1 hour (to measure p65 and CREB1 activation) or 3 hours (to measure c-Jun activation). The mean fluorescence intensify (MFI) values for the indicated phosphoproteins were determined by flow cytometry The *P* values obtained by the Kruskal-Wallis test are indicated above the error bars, which correspond to the SEM. Each experiment was repeated at least three times with independent biological samples.